Journal of Catalysis **202,** 34–44 (2001)
doi:10.1006/jcat.2001.3242, available online at http://www.idealibrary.com on IDEAL®

Oxidation of CO on a Pt/Al_2O_3 Catalyst: From the Surface Elementary Steps to Light-Off Tests

I. Kinetic Study of the Oxidation of the Linear CO Species

Abdennour Bourane and Daniel Bianchi[1]

Laboratoire d'Application de la Chimie à l'Environnement (LACE), UMR 5634, Université Claude Bernard, Lyon-I, Bat. 303, 43 Bd du 11 Novembre 1918, 69622 Villeurbanne, France

Received September 18, 2000; revised March 29, 2001; accepted April 2, 2001

The adsorption of CO (1% CO/He mixture) at 300 K on a 2.9% Pt/Al_2O_3 catalyst leads to the detection of a strong IR band at 2075 cm^{-1} associated with a weak and broad IR band at $\approx$1850 cm^{-1} ascribed to linear (denoted by L) and multibound (Bridged and 3-fold coordinated) CO species, respectively. Due to a high heat of adsorption, the L species does not desorb in helium at a temperature lower than 350 K. This allows us to study the rate of oxidation of the L species using several x% O_2/He mixtures (x in the range 0.5–100) and at five reaction temperatures (range 298–350 K). It is shown that the L species is oxidized into CO_2 according to the elementary step (denoted by S3): $L + O_{ads} \rightarrow CO_2$ (rate constant k_3) involving a dissociatively adsorbed oxygen species. The change in the rate of disappearance of the L species (determined by the evolution of its coverage θ_L) with the O_2 partial pressure (P_{O_2}) indicates that the reaction proceeds (a) without any competition between L and O_{ads} species; and (b) with an apparent rate constant k_a which varies linearly with $P_{O_2}^{0.5}$. This indicates that O_{ads} is weakly adsorbed with a coverage (denoted by θ_o) given by Langmuir's model for dissociative chemisorption: $\theta_o = (K_{O_2}P_{O_2})^{0.5}$ with $(K_{O_2}P_{O_2})^{0.5} \ll 1$. The apparent rate constant of step S3 determined at several reaction temperatures leads to an apparent activation energy $E_a = E_3 - (E_{O_2}/2) = 65 \pm 3$ kJ/mol (where E_3 is the activation energy of step S3 and E_{O_2} is the heat of adsorption of oxygen). It is shown that the preexponential factor of the apparent rate constant is in agreement with the value expected from the statistical thermodynamics considering immobile adsorbed species. Moreover, when one considers that the oxygen is weakly adsorbed even with $P_{O_2} = 10^5$ Pa, it is shown that E_{O_2} must be $<\approx$30 kJ/mol, leading to an activation energy E_3 in the range 65–80 kJ/mol. The rate of oxidation of the L species characterized by step S3 allows us to interpret in following studies the data (coverage of the L species and CO conversion) recorded during the light-off tests using several 1% CO/x% O_2/He mixtures with x in the range 0.125–50.

1. INTRODUCTION

One of the objectives in gas/solid catalysis is to correlate the rate of appearance of the products of a given catalytic reaction to the elementary steps on the surface of the catalyst. This is done with the hope that by determining the elementary steps which control the appearance of the product, it is possible to modify these steps to improve the conversion or the selectivity. The catalytic oxidation of CO on supported noble metal catalysts is one of the most simple and widely studied catalytic reactions. However, the correlation between elementary steps and rate of CO_2 production is still debated (1, 2). One of the classical methods of correlating elementary steps and rate of reaction is to perform a kinetic study under isothermal conditions, determining the effect of the partial pressures of the reactants and products on the rate of reaction as it was done, for instance, by Nibbelke *et al.* (1), Herz and Marin (3), and Harold and Garske (4) for the CO/O_2 reaction on Pt/Al_2O_3 catalysts. The experimental curves are then compared to those expected from elementary step reaction paths to determine several kinetic parameters (1, 3, 4). This procedure is time consuming and the studies are particularly difficult for exothermic reactions as the oxidation of CO (2 and references therein). This explains that nowadays it is common to characterize a catalytic reaction such as CO/O_2 by light-off tests which consist of following either the conversion of the reactant CO or the appearance of the product CO_2 during an increase of the reaction temperature (2, 5, 6). Then, the curves can be compared to kinetic models to extract by optimization some kinetic constants (2, 4).

In parallel to the above studies, numerous works on various noble metal-containing solids (single crystals, model particles, supported metal catalysts) have the objective of studying the individual elementary steps involved in the CO/O_2 reaction. These studies have been reviewed by several authors such as Engel and Ertl (7) and Razon and

[1] To whom correspondence should be addressed. E-mail: daniel.bianchi@univ-lyon1.fr.

0021-9517/01 $35.00

Schmitz (8) (see also Ref. 2). Razon and Schmitz (8) particularly considered the studies related to the oscillation phenomena but gave a large review of the elementary steps proposed for the CO/O_2 reaction on noble metal-supported catalysts. Engel and Ertl (7) summarized the contribution of UHV studies on single crystals to understand the CO/O_2 reaction. It seems now clearly proven that the Langmuir-Hinshelwood mechanism between adsorbed CO and an oxygen species (denoted by O_{ads}) coming from the dissociative chemisorption of O_2 explains most experimental results under UHV conditions (7). However, there are several aspects of the reaction which are still debated (1, 2), in particular the pressure gap between UHV conditions (i.e., CO pressure $<\approx 10^{-4}$ Pa (7)) and real conditions in applied catalysis (CO pressure $>10^2$ Pa). For instance, on Pt(110) at a total pressure of 2.6×10^{-5} Pa, with a ratio $P_{O_2}/P_{CO} = 1.3$ (7), the profile of the rate of the CO_2 production with the reaction temperature T_r reveals a maximum at $T_m \approx 473$ K and this value increases with the partial pressure of CO. This profile also observed for Pd(111) is explained (7) considering that for $T_r < T_m$ the coverage of the adsorbed CO decreases with the increase in T_r due to the adsorption equilibrium. This liberates some sites for the adsorption of oxygen. For $T_r > T_m$ the rate of CO_2 decreases because the coverage of CO continues to decrease. The above views of the CO/O_2 reaction on single crystals have been confirmed in particular on Pt(111) (9) and Pd(110) (10). On single crystals, the heat of adsorption of CO appears as a key parameter in the interpretation of the rate of the CO_2 production, considering that it fixes the coverage of the adsorbed CO species for a given CO partial pressure and reaction temperature. Using Infrared reflection absorption spectroscopy (IRAS) combined with kinetic studies, Szanyi and Goodman (11) confirmed on Pd(100) that there is a close correlation between the heat of adsorption of CO and the apparent activation energy of the reaction.

In previous studies (12–18), we have shown that an analytical procedure using FTIR spectroscopy might allow us to perform on supported metal catalysts experiments similar to those done with IRAS on single crystals and model particles but at a higher total pressure (1 atm) and in a large temperature range of (300–900 K). For instance, this procedure has been used for the determination of the heats of adsorption of the linear (denoted by L) (12, 13) and bridged (denoted by B) (19) CO species formed on a 2.9% Pt/Al_2O_3 catalyst, as a function of the coverage of each species. For the L species which dominate the FTIR spectra, the heat of adsorption varies linearly with its coverage (denoted θ_L) from $E_1 = 115$ kJ/mol at $\theta_L = 1$ to $E_0 = 206$ kJ/mol at $\theta_L = 0$ (11, 12). These values indicate that at 550 K, θ_L is still equal >0.99 at a CO partial pressure of 10^3 Pa, commonly observed in three-way catalysis. Moreover, we have shown (20) that at a constant partial pressure of CO (10^3 Pa), θ_L (and consequently the heat of adsorption) is not significantly modified in the presence of a coadsorbed species in particular O_2 with a CO/O_2 ratio >2. It is well known that on Pt/Al_2O_3 catalysts the formation of CO_2 during a light-off test is detected with a 1% CO/x% O_2/inert gas reactive mixture at a temperature significantly lower than that needed to strongly decrease the coverage of the L species (2–4). This leads to the conclusion that it is not necessary to consider that the L species must quantitatively desorb to increase the rate of CO_2 production. Note that the heats of adsorption of the L species (12, 13) indicate that θ_L decreases at around 380 K at a CO partial pressure of 10^{-4} Pa (UHV conditions) and this fact agrees well with the interpretation of the evolution of the rate of CO_2 production on single crystals (7, 9–11).

The above discussion has shown that the pressure gap between single crystals and supported metal catalysts studies can lead to a new insight on the CO/O_2 reaction. Moreover, the diversity of adsorption sites (various steps, terraces, and defects) on the Pt particles of the supported catalysts, as compared to a single crystal, may also lead to some differences in the mechanism of the CO/O_2 reaction on the two types of solids. The studies on single crystals have indeed shown that the heat of adsorption of the CO species is a crucial parameter for interpreting the data on the CO/O_2 reaction (7, 9–11). Moreover, the heats of adsorption of L and B species on several supported metal catalysts (12–19 and references therein) can be strongly different especially on Pt (11, 12, 19). This leads to the conclusion that to obtain more insight on the CO/O_2 reaction on Pt-supported catalysts, it is necessary to study the contribution of each adsorbed species (L and B) for the CO_2 production as considered by several authors (21–25). We consider the involvement of the L CO species on the rate of oxidation of CO on a 2.9% Pt/Al_2O_3 catalyst. The mechanism for the oxidation of CO via the L species is considered as follows (Model I) (1–7):

Step S1: Formation of the L species $CO_{(gas)} \Leftrightarrow L$.
Step S2: Dissociative chemisorption of oxygen $O_{2(gas)} \Leftrightarrow 2\,O(ads)$.
Step S3: Oxidation of the L species $L + O_{(ads)} \rightarrow CO_{2(ads)}$.
Step S4: Desorption of CO_2 $CO_{2(ads)} \rightarrow CO_{2(gas)}$.

The above mechanism can be used to derive an expression for the rate of disappearance of CO, and then by optimizing the experimental data, to determine some kinetic parameters. This is a procedure followed in numerous studies (1–4, 26). We adopt a slightly different approach. In a first step, we study each elementary step S1 to S4, of the above mechanism determining the fundamental kinetic parameters (heats of adsorption, activation energy, preexponential factor). Then these parameters are used to compare the experimental curves (coverage of the L species and CO conversion) recorded during light-off tests using several CO/O_2/He mixtures and the theoretical curves expected

from the above Model I. This approach of the correlation between elementary steps and data recorded during light-off experiments presents the advantage of limiting the number of unknown parameters for the optimization procedure engaged between model and experimental data.

Step S1 has been characterized previously (12, 13, 19), determining the heats of adsorption of the L species at several coverages. Moreover, we have shown (20) that these values are not significantly modified in the presence of several gases in particular O_2 (for CO/O_2 ratios >2), CO_2, and H_2O. Step S4 is considered fast for $T > 300$ K (7). Note that step S2 is an equilibrium in the above mechanism that is different in several studies (7, 8). However, Razon and Schmitz (8) indicate six kinetic models for the oxidation of CO on platinum which consider that step S2 is an equilibrium. The kinetic study of step S3 (kinetic order, apparent rate constant, and activation energy) and correlatively of step S2 constitute the objective of the present study. This is performed by studying the effect of the oxygen partial pressure on the rate of disappearance of the L species (preadsorbed on Pt/Al_2O_3) in the course of its oxidation at $T_r < 350$ K.

2. EXPERIMENTAL

The 2.9% Pt/Al_2O_3 (in wt%) catalyst was the same as that used in previous studies (12, 13, 19). It was prepared by the incipient wetness method. Alumina (Degussa C γ-Al_2O_3, BET area 100 m^2/g) was impregnated using an amount of aqueous solution of H_2PtCl_6, xH_2O ($\approx$1.1 cm^3/g of alumina). After drying for 12 h at room temperature and then for 24 h at 373 K, the solid was treated for 12 h in air at 713 K. The noble metal content was obtained using the inductively coupled plasma method after dissolution of the catalyst powder with acid solutions (in particular HNO_3, HF, and HCl). For the FTIR study, the catalyst was compressed to form a disk ($\phi = 1.8$ cm) which was placed in the sample holder of a small internal volume stainless-steel IR cell (transmission mode) described elsewhere (12). This IR cell enabled *in situ* treatments (293–900 K) of the solid, at atmospheric pressure, with a gas flow rate in the range of 150–2000 cm^3/min. Before the adsorption of CO, the solid was treated *in situ* (150 cm^3/min) according to the following procedure: oxygen ($T = 713$ K, $t = 30$ min) $\rightarrow$ helium ($T = 713$ K, $t = 30$ min) $\rightarrow$ hydrogen ($T = 713$ K, $t = 1$ h) $\rightarrow$ helium ($T = 713$ K, $t = 10$ min) $\rightarrow$ helium (adsorption temperature). After this treatment, the dispersion of the metallic phase of the reduced fresh catalyst was 85% (12, 13, 19), in agreement with literature data (27) on similar Pt catalysts. The same catalyst pellet was used for several experiments and it was pretreated before each adsorption experiment as described above.

The oxidation of the L species was studied according to the following procedure: after the pretreatment of the catalyst, CO was adsorbed at 300 K with a 1% CO/He mixture (200 cm^3/min) and then a switch 1% CO/He $\rightarrow$ x% O_2/He (200 cm^3/min) was performed with x in the range 0.5–100 while the IR spectra of the adsorbed CO species were periodically recorded. Similar experiments were performed at several temperatures all lower than 350 K. We ascertained the repeatability of the results (value of the apparent rate constants) on the oxidation of the L species performing the following experiment: pretreated solid $\rightarrow$ 1% CO/He $\rightarrow$ x% O_2/He $\rightarrow$ 1% CO/He $\rightarrow$ x% O_2/He. We observed no differences in the apparent rate constant of oxidation between the first oxidation and the second or further experiments. All the experiments described in the present study were obtained after at least one cycle 1% CO/He $\rightarrow$ x% O_2/He.

Some experiments were run with an analytical system designed for transient experiments using a mass spectrometer as a detector and previously described (12). With the help of various valves we performed switches between regulated gas flows (1 atm total pressure) which passed through a catalyst (powder) contained in a quartz microreactor. A quadrupole mass spectrometer permitted the determination of the composition (molar fraction) of the gas mixture at the outlet of the reactor during a switch, after a calibration procedure.

3. RESULTS AND DISCUSSION

3.1. Oxidation of the L Species

Figure 1 gives the evolution of the FTIR spectra during the switch 1% CO/He $\rightarrow$ 2% O_2/He at 298 K on the

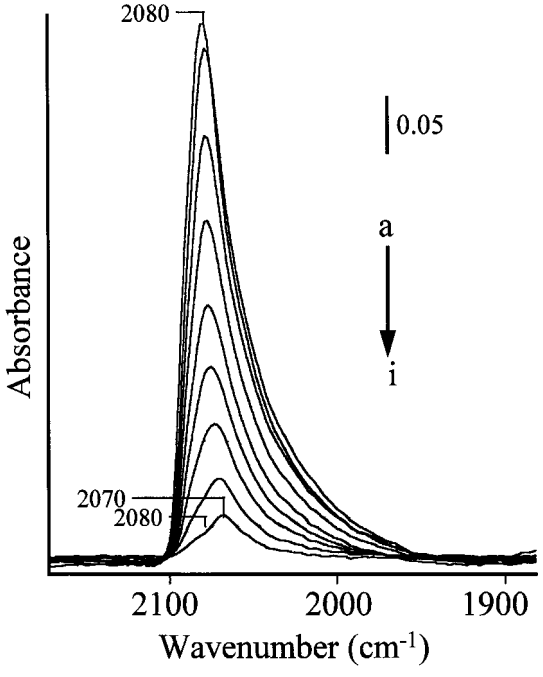

FIG. 1. Evolution of the IR band of the L species adsorbed on 2.9% Pt/Al_2O_3 with the duration of the oxidation with 2% O_2/He at 298 K: (a–i) 30, 50, 62, 74, 87, 100, 118, 154, 217 s.

Pt/Al_2O_3 catalyst. The IR band of the L species is observed at 2080 cm^{-1} in the presence of CO/He while on a fresh reduced solid it is observed at 2075 cm^{-1} (12, 13). This is due to the presence of oxygen on the surface coming from the first cycle 1% CO/He → 2% O_2/He in agreement with several studies (28, 29), and references therein. It can be observed that the intensity decreases progressively with time on stream associated to a shift of the IR band to lower wavenumbers: 2078, 2073, 2070 cm^{-1} after 62, 118, and 217 s in 2% O_2/He, respectively, while the corresponding coverages are 0.84, 0.25, 0.06 (see below the determination of the coverage). At low coverage, a shoulder at 2080 cm^{-1} is detected (Figs. 1h–j). In the absence of O_2, the IR band remains constant (no desorption) in agreement with the high heat of adsorption of the L species $E_1 = 115$ kJ/mol at $\theta = 1$ (11, 12). A similar experiment performed with the quartz microreactor indicates that only CO_2 is formed during the switch 1% CO/He → 2% O_2/He at 298 K. This confirms that there are (a) no CO desorption during the oxidation of the L species; (b) no competition between the L species and adsorbed oxygen; and (c) no significant decrease in the heat of adsorption of the L species in the presence of O_2. These conclusions are in agreement with a previous study which has shown that the heat of adsorption of CO was not modified in the presence of O_2 with a CO/O_2 ratio >2 (20). Figure 2 gives the IR spectra during an experiment similar to that described in Fig. 1 but for a higher O_2 partial pressure 1% CO/He → 8% O_2/He at 298 K. It can be observed in Fig. 2 that: (a) the IR band disappears faster with a higher O_2 pressure; (b) the IR band shifts with the decrease in coverage (2070 cm^{-1} after 151 s, $\theta_L = 0.12$); and (c) a shoulder is detected at 2080 cm^{-1} at low coverages (Figs. 2h–2j). Note that the shift (≈ -10 cm^{-1}) of the IR band with the coverage observed in Figs. 1 and 2 during the oxidation of the L species is lower than the one (≈ -25 cm^{-1}) measured during an adsorption procedure at high temperatures (12) in agreement with the observations of Sarkany *et al.* (28). We performed similar experiments with 0.5 and 16% O_2/He mixtures and with pure O_2. The evolutions of the IR spectra with time on stream did not reveal strong differences with the results in Figs. 1 and 2. However, with pure oxygen, the shoulder at 2080 cm^{-1} observed at low coverages in Figs. 1 and 2 is detected at higher coverages as shown in Fig. 3. Note that for P_{O_2} > 8000 Pa a small IR band is detected at 2120 cm^{-1} (Fig. 2) ascribed to linear CO species adsorbed on Pt^{2+} (22, 23, 25). This indicates that few Pt^0 sites are converted into Pt^{2+} during the first oxidation. The increase in P_{O_2} does not change the intensity of this IR band (Fig. 3). Moreover, this linear CO species is not oxidized at 298 K as shown in Fig. 2. Figure 4 gives the evolution of the coverage, θ_L in the range 1–0.2 with time on stream in x% O_2/He ($x = 0.5$, 2, 8, 16, 100). The θ_L values are determined considering that the IR band area are proportional to the amount of L species on the surface as studied previously (12, 30), θ_L = (IR band area at t)/(IR band

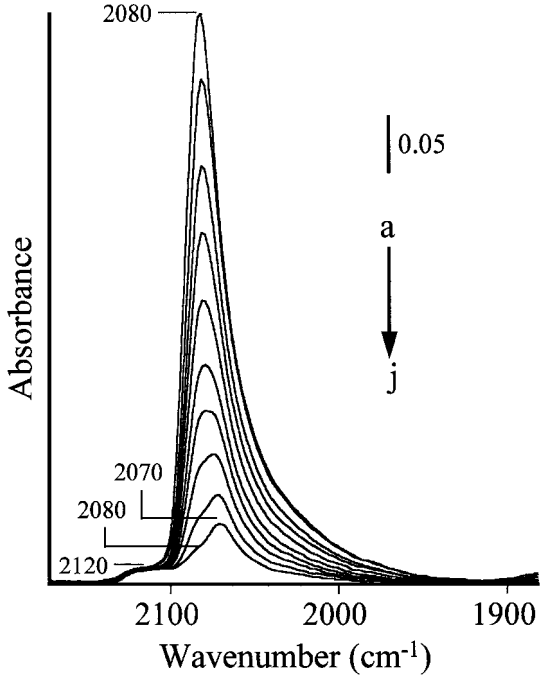

FIG. 2. Evolution of the IR band of the L species adsorbed on 2.9% Pt/Al_2O_3 with the duration of the oxidation with 8% O_2/He at 298 K: (a–j) 6, 12, 23, 32, 42, 53, 63, 79, 106, 151 s.

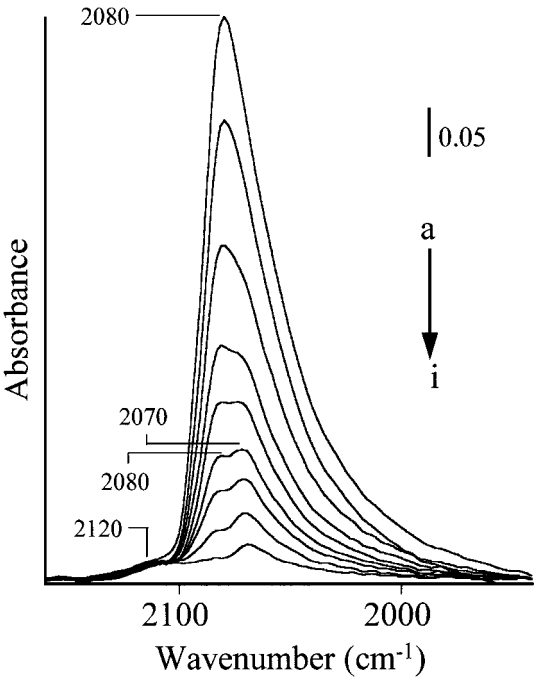

FIG. 3. Evolution of the IR band of the L species adsorbed on 2.9% Pt/Al_2O_3 with the duration of the oxidation with pure O_2 at 298 K: (a–i) 0, 5, 9, 13, 15, 19, 23, 30, 52 s.

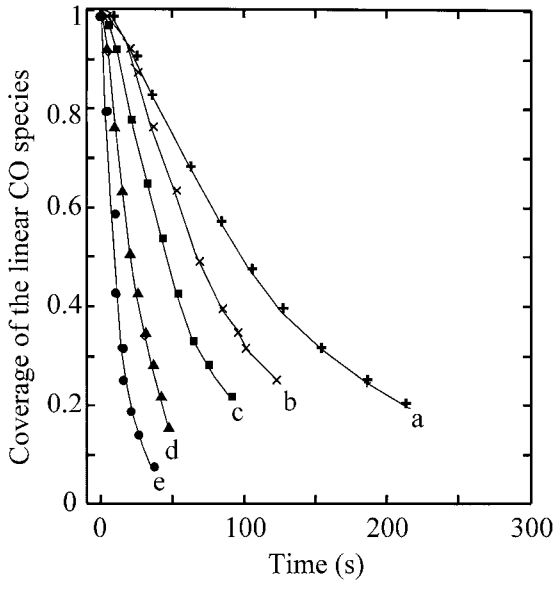

FIG. 4. Evolution of the coverage of the L species with the duration of the oxidation for several oxygen partial pressures in Pa: (a) 5×10^2; (b) 2×10^3; (c) 8×10^3; (d) 16×10^3; (e) 10^5.

area at $t = 0$). The shoulder at 2080 cm^{-1} and the main IR band are not differentiated. We comment below the evolutions of θ_L for values lower than ≈0.2, taking into account the results published by Cant and Donaldson (31) on the oxidation of the L species at similar coverages.

The curves in Fig. 4 are used to determine the kinetic parameters of the oxidation of the L species according to step S3.

3.2. On the Absence of Competition between L and Adsorbed Oxygen Species

We observe no change in the IR band intensity during a switch 1% CO/He → He indicating that the L species does not desorb in an inert atmosphere. This agrees with the theoretical rate of desorption obtained from the heat of adsorption values. Considering that the activation energy of desorption $E_d(\theta_L)$ is equal to the heat of adsorption which varies linearly from 206 kJ/mol at $\theta = 0$ to 115 kJ/mol at $\theta = 1$ (12, 13), the rate of desorption of the L species is given by (first kinetic order)

$$\frac{-d\theta_L}{dt} = \frac{k \cdot T}{h} \cdot \exp\left(-\frac{E d(\theta_L)}{R \cdot T}\right) \cdot \theta_L, \qquad [1]$$

where k is Boltzmann's constant, h is planck's constant, T is the desorption temperature, and R is the gas constant. Numerical calculations show that there is no desorption of the L species at 300 K. Moreover the heat of adsorption of the L species is not modified in the presence of O_2 (20) for CO/O_2 ratios >2. This means that we cannot adopt the view that the L species must desorb to liberate some sites for the adsorption of oxygen. It must be considered either that there are some free sites (other than those adsorbing the L species) on the Pt particles which activate oxygen or that the L species is oxidized by a Eley-Rideal mechanism (denoted by E-R) and not by a L-H mechanism. We show below that the E-R mechanism is improbable. Another fact proves that there is no competition between L species and adsorbed oxygen.

The rate of disappearance of the L species during the oxidation according to step S3 is given by

$$\frac{-d\theta_L}{dt} = k_3 \cdot \theta_L \cdot \theta_0, \qquad [2]$$

with θ_O being the coverage of the oxygen species. Assuming a competition on the same sites $\theta_O = (1 - \theta_L)$ then Eq. [2] leads to the conclusion that the rate of disappearance of the L species is maximum at $\theta_L = 0.5$. Curve b in Fig. 5 shows the evolution of the rate $v = -d\theta_L/dt$ with time on stream for the experiment with the 16% O_2/He mixture. Similar curves are obtained for the various O_2 partial pressures. Curve b in Fig. 5 shows clearly that the rate is maximum just after the time required to obtain the O_2 adsorption equilibrium after the switch 1% CO/He → 16% O_2/He for a θ_L value clearly higher than 0.5 (curve a in Fig. 5). There are several studies which describe the oxidation of preadsorbed CO species by O_2-containing gas mixtures, on noble metal-supported catalysts and at temperatures lower than 400 K (26, 32). The authors (26, 32) observe that the introduction of O_2 leads to the immediate production of CO_2 with a rate showing a maximum at Time 0 and decreasing with time on stream. A clearly different situation is observed,

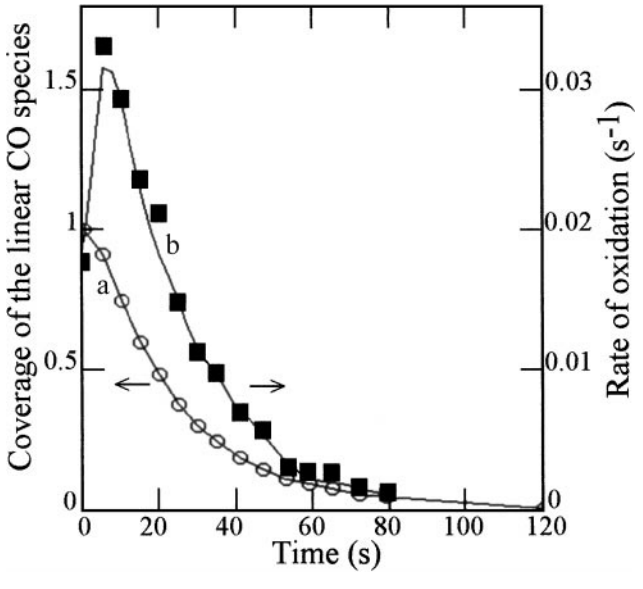

FIG. 5. Evolution of the coverage of the L species and of the rate of oxidation for the 16% O_2/He mixture: (a) coverage; (b) rate of oxidation.

for instance, on Pd(110) (10). For a CO coverage >0.64, the introduction of O_2 does not lead to the formation of CO_2 (O_2 cannot be adsorbed) while for a coverage of 0.46, the rate of CO_2 production increases slowly with the duration of oxidation until a maximum is observed after 200 s at 310 K (10). For a coverage of 0.1 the rate is maximum immediately (10). It must be noted that the results in Fig. 5 are different from those of Li *et al.* (33) on Pt/SiO_2. At 353 K, these authors (33) observed that the IR band of the L species rapidly decreases only after an induction period of 109 s after the introduction of O_2.

It seems clearly established that L and O_{ads} species on the present Pt/Al_2O_3 catalyst are not adsorbed on the same sites. This is in agreement with the observations of Xu and Yates (34) on Pt (335). Using IRAS they have shown that the more reactive geometry in the CO/O_2 reaction involves oxygen adsorbed on step sites with CO adsorbed on terrace sites. Their results indicate that two types of adsorption sites can be involved in the adsorption of CO and O_2, a conclusion which is also found from the present results on Pt/Al_2O_3 and this is related to the diversity of the sites which may exist on supported Pt particles.

3.3. *Influence of the Partial Pressure of O_2 on the Rate of Oxidation of the L Species*

Assuming that during the oxidation of the L species, θ_0 is constant with the duration of the adsorption t, the expression [2] leads to the conclusion that $\ln \theta_L$ must linearly vary with t. Figure 6 shows the curves $\ln \theta_L = f(t)$ obtained from the data in Fig. 4. The straight lines observed in Fig. 6 for several P_{O_2} values confirm that θ_O does not significantly change during the oxidation of the L species. The slopes of the straight lines give the apparent rate constants of step S3, $k_{ap} = k_3\theta_O$, for each O_2 partial pressure. Note that the fact that the slopes in Fig. 6 change with the partial pressure of O_2 leads to the conclusion either that O_2 is not strongly adsorbed or that the oxidation follows the E-R mechanism. Considering Langmuir's model, θ_O is given by

$$\theta_O = \frac{\sqrt{K_{O_2} \cdot P_{O_2}}}{1 + \sqrt{K_{O_2} \cdot P_{O_2}}}, \qquad [3]$$

where K_{O_2} and P_{O_2} are the adsorption coefficient and the partial pressure of O_2, respectively. If the heat of adsorption of oxygen is high, (a) $(K_{O_2}P_{O_2})^{0.5} \gg 1$; (b) θ_O is independent of the O_2 partial pressure; and (c) k_{ap} must be independent of P_{O_2}. This situation is not observed during the oxidation of the L species. This is surprising because it is well known that the heats of adsorption of oxygen on noble metal-containing solids are very high in particular with Pt. They are in the range 186–289 kJ/mol in (35) and Wartnaby *et al.* (36) consider that on Pt(110) the heats of adsorption of oxygen alone decrease with the increase in the coverage from 335 ± 10 kJ/mol at low coverages to 214 ± 24 kJ/mol at 0.35 ML and 199 ± 27 kJ/mol at 0.5 ML. These values indicate that oxygen must be strongly adsorbed and that the coverage must be equal to $\theta_O = 1$ at temperatures lower than 350 K. The variation of the apparent rate constant (Fig. 6) with P_{O_2} shows that the heat of adsorption of oxygen is strongly decreased in the presence of adsorbed CO. This is in agreement with several studies on Pt- and Pd containing solids (single crystals and supported metal catalysts) which show that at room temperature CO preferentially adsorbs even with O_2-rich CO/O_2 mixtures and that CO adsorption is not significantly affected by the O_2 adsorption (11, 21, 24, 25, 31).

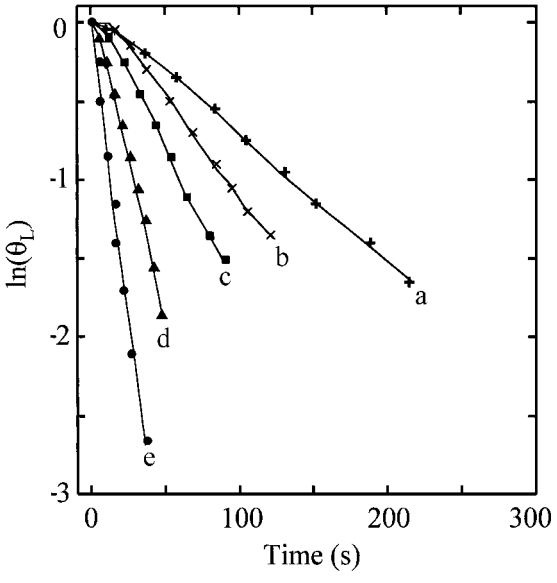

FIG. 6. Evolution of the curves $\ln(\theta_L) = f(t)$ during the oxidation of the L species for the various oxygen partial pressure in Pa: (a) 5×10^2; (b) 2×10^3; (c) 8×10^3; (d) 16×10^3; (e) 10^5.

In our experiment, it cannot be ruled out that during the first switch 1% CO/He → x% O_2/He, some oxygen is adsorbed on Pt sites with a high heat of adsorption (strongly adsorbed oxygen species). For instance, Sarkany *et al.* (28) performed the titration of the L species adsorbed on a Pt/SiO_2 catalyst by introduction of oxygen pulses (100 μl) at 298 K. They determined by O mass balance that during the first pulse 25% of O_2 did not react, 40% reacted with the L species to form CO_2, and 35% was adsorbed (28). However, these eventual strongly adsorbed O_{ads} species are not active in the oxidation of the L species. This is shown by the experiments in Fig. 7. After that the coverage of the L species was decreased by oxidation using a 16% O_2/He mixture; a switch 16% O_2/He → He is performed at $\theta_L \approx$ 0.4. It can be observed that the coverage of the L species remains constant just after the removal of the oxygen in the gas phase. After a switch He → 16% O_2/He the coverage decreases again and the oxidation ceases after a new switch 16% O_2/He → He at $\theta \approx 0.15$. This clearly shows

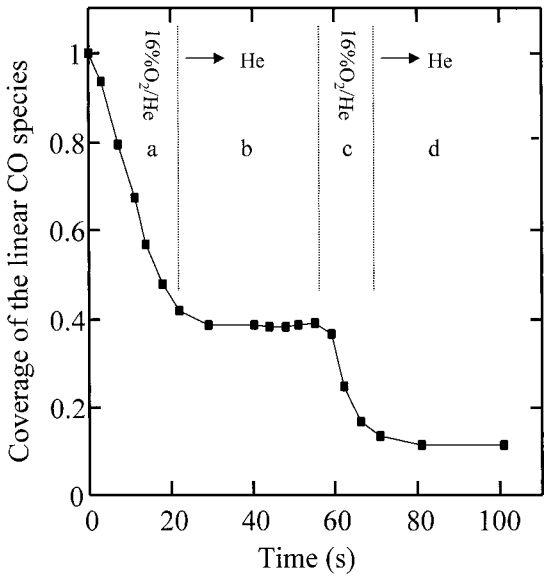

FIG. 7. Evolution of the coverage of the L species during several switches 16% O_2/He → He → 16% O_2/He.

that the oxidation of the L species cannot involve some strongly adsorbed oxygen species. The reaction involves either a weakly adsorbed oxygen species or O_2 from the gas phase by a E-R mechanism. Note that the introduction of O_2 in section c of Fig. 7 leads to an initial rate of oxidation of the L species slightly higher than that before the switch O_2/He → He. We believe that this is due to the heat coming from the O_2 adsorption.

3.4. *Mechanism of the Oxidation of the L Species*

The slopes of the straight lines in Fig. 6 give the apparent rate constant of the oxidation of the L species, $k_{ap} = k_3\theta_O$, for each O_2 partial pressure. These slopes changes with P_{O_2} and this must be due either to an E-R mechanism (in that case $k_{ap} = k_3 P_{O_2}$) or to a L-H mechanism with an oxygen species weakly adsorbed. The choice between the two mechanisms can be made by studying the variation of the apparent rate constant with P_{O_2}. For the L-H mechanism, assuming that $(K_{O_2}P_{O_2})^{0.5} \ll 1$, $\theta_O = (K_{O_2}P_{O_2})^{0.5}$, which indicates that at a given reaction temperature $k_{ap} = f(P_{O_2}^{0.5})$ must vary linearly as observed in Fig. 8 (■). For the E-R mechanism $k_{ap} = f(P_{O_2})$ must be a straight line. Figure 8 (○) shows that $k_{ap} = f(P_{O_2})$ is not a straight line in the P_{O_2} range 0.5×10^3–10^5 Pa and that the E-R mechanism must be discarded. However, it can be observed that $k_{ap} = f(P_{O_2})$ is roughly a straight line for P_{O_2} lower than 10^4 Pa. This means that the experiments done with $P_{O_2} < 10^4$ Pa may not allow us to discriminate between a L-H mechanism with O_2 weakly adsorbed and an E-R mechanism (or another mechanism leading to an order 1 for P_{O_2}: i.e., the molecular adsorption of O_2 considered as the rate-determining step (1)). Figure 8 (■) indicates that the apparent rate constant k_{ap} linearly varies with $P_{O_2}^{0.5}$: $k_{ap} = k'_{ap}P_{O_2}^{0.5}$ with $k'_{ap} = k_3(K_{O_2})^{0.5}$ a new apparent rate constant equal to 2.8×10^{-4} $Pa^{0.5}$ s^{-1} at 300 K. Curve c in Fig. 8 reports the theoretical straight line $k_{ap} = 2.8 \times 10^{-4}\ P_{O_2}^{0.5}$, while curve d represents $Y = (2.8 \times 10^{-4}\ P_{O_2}^{0.5}) = f(P_{O_2})$ in order to confirm the necessity of using oxygen partial pressures higher than 10^4 Pa to select the mechanism of oxidation of the L species.

Assuming immobile adsorbed oxygen species, the adsorption coefficient K_{O_2} is given by statistical thermodynamics (37, 38),

$$K_{O_2} = \frac{h^3}{k * (2 * \pi * m * k)^{3/2}} * \frac{1}{T_a^{5/2}} * \exp\left(\frac{E_d - E_a}{R * T_a}\right), \quad [4]$$

where m is the weight of the molecule (32×10^{-3} kg/6.02×10^{23}), T_a is the adsorption temperature, E_d and E_a are the activation energies of desorption and adsorption, respectively, and $E_{O_2} = E_d - E_a$ is the heat of adsorption of O_2. To maintain the relation $(K_{O_2}P_{O_2})^{0.5} \ll 1$ even with a partial pressure of O_2 of 10^5 Pa, E_{O_2} must be lower than ≈30 kJ/mol which leads to $(K_{O_2}\ 10^5)^{0.5} = 0.086$. This E_{O_2} value is strongly lower than that determined in the absence of CO (>180 kJ/mol) (35, 36).

3.5. *Apparent Activation Energy for the Oxidation of the L Species*

Figure 9 gives the evolution of the IR band of the L species with a 2% O_2/He mixture at 321 K. The spectra are similar to those in Fig. 1 but the IR band decreases faster at

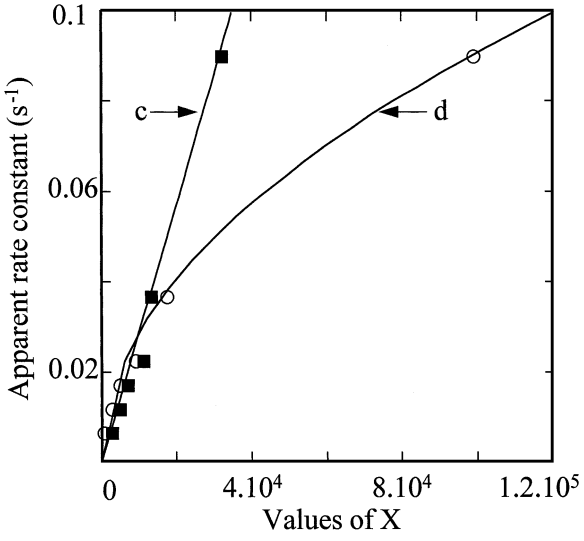

FIG. 8. Choice of the mechanism for the oxidation of the L species ($X = P_{O_2}^{0.5}$ or P_{O_2}): (■, a) experimental data, $k_{ap} = f(P_{O_2}^{0.5})$; (○, b) experimental data, $k_{ap} = f(P_{O_2})$;(c) theoretical curve $k_{ap} = 2.8 \times 10^{-4} P_{O_2}^{0.5}$; and (d) theorectical curve $(2.8 \times 10^{-4} P_{O_2}^{0.5}) = f(P_{O_2})$.

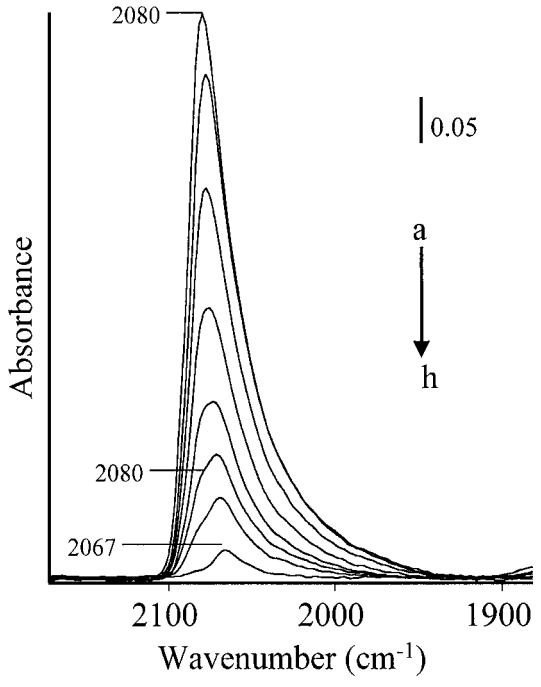

FIG. 9. Evolution of the IR band of the L species adsorbed on 2.9% Pt/Al_2O_3 with the duration of the oxidation with 2% O_2/He at 321 K: (a–h), 33, 44, 48, 51, 55, 59, 65, 73 s.

321 K. Note that the IR band of the L species shifts to lower wavenumbers with the decrease in coverage from 2080 to 2067 cm^{-1}. We have performed similar experiments at five temperatures with the same 2% O_2/He mixture. This allows us to determine the evolution of the apparent rate constant of step S3 with the reaction temperature. Figure 10 gives ln $k_{ap} = f(1/T)$ for $P_{O_2} = 2 \times 10^3$ Pa and the straight line leads to the apparent activation energy $E_a = (E_3 - (E_{O_2}/2)) = 65 \pm 3$ kJ/mol. As the heat of adsorption of O_2 is estimated to be ≈30 kJ/mol or lower, the activation energy E_3 of step S3 is in the range 65 ± 3 to $\approx 80 \pm 3$ kJ/mol. The above values for the activation energies E_a and E_3 can be compared to literature data. We show below that E_a is in good agreement with the values determined by Cant and Donaldson (31) on Pt/SiO_2 from experimental data similar to those obtained in the present study. The values of E_3 can be compared to the activation energy E_{SR} of the surface reaction $CO_{ads} + O_{ads}$ involved in L-H kinetic models of the CO/O_2 reaction on various Pt-containing solids. For instance on a Pt foil at $T > 750$ K and for CO/O_2 ratios <1, Coulston and Haller (39) determined $E_{SR} = 65$ kJ/mol. On Pt/Al_2O_3 at $T \approx 473$ K, Herz and Marin (3) found $E_{SR} = 56.5$ kJ/mol while on $Pt/Rh/CeO_2/Al_2O_3$ at 393–433 K Nibbelke *et al.* (26) determined 96.8 kJ/mol. This value is similar to that determined by Pacia *et al.* (40) on a Pt ribbon: 91 kJ/mol. Engel and Ertl (7) pointed out that low values of E_{SR} could be due to the simplifying assumptions involved in the kinetic models. The above values of E_{SR} are in reasonable agreement with E_3 determined in the present study for the oxidation of the L CO species.

3.6. Preexponential Factor for the Apparent Rate Constant of Step S3

The straight line in Fig. 10 gives a preexponential factor for k_{ap} of 11×10^8 s^{-1} at $P_{O_2} = 2\ 10^3$ Pa. This value can be compared to the theoretical value expected from statistical thermodynamics considering $k_{ap} = k_3(K_{O_2} * P_{O_2})^{0.5}$. The adsorption coefficient is given by expression [4]. It can be denoted as $K_{O_2} = (K_{O_2})_0 \exp(E_{O_2}/RT)$, with $(K_{O_2})_0$ the preexponential factor. The rate constant of step S3 is given by $k_3 = A_3 \exp(-E_3/RT)$. The preexponential factor of a bimolecular reaction as step S3 is $A_3 = kT/h \approx 10^{13}$ s^{-1} (3, 26, 37, 38). The theoretical preexponential factor of the apparent rate constant of steps S3 is $A_3\ ((K_{O_2})_0 P_{O_2})^{0.5} \approx 4 \times 10^8$ s^{-1} at 300 K. The very good agreement between this value and that determined experimentally can be observed. This confirms that step S3 involves the strongly adsorbed L species with a weakly dissociatively adsorbed oxygen species.

From the above calculation it can be considered that the rate constant k_3 of step S3 has a preexponential factor of 10^{13} s^{-1} at $T < 350$ K, with an activation energy of E_3 in the range 65–80 kJ/mol.

3.7. Rate of Oxidation of the L Species and CO Conversion during a Light-Off Test

A simple relationship can be established between the oxidation of the L species and the conversion of CO during a light-off test. It may appear surprising that the L species is oxidized at room temperature for instance with 2% O_2/He (Fig. 1) while the conversion is not detected at a significant level before ≈400 K during a light-off tests

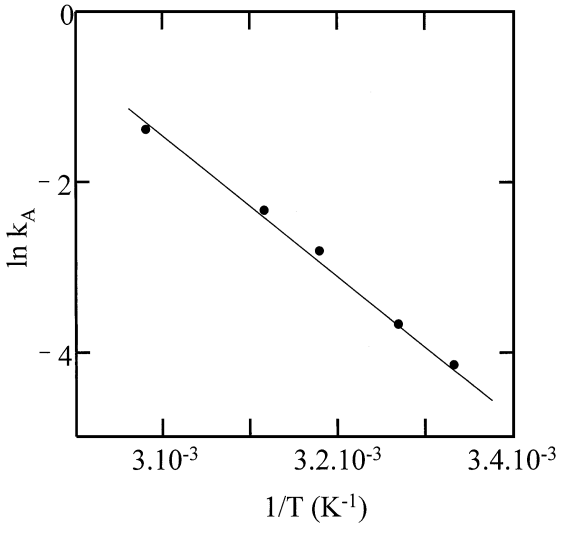

FIG. 10. Determination of the apparent activation energy for step S3.

with 1% CO/2% O_2/He performed with the FTIR cell (results not shown). Similar observations were made by several authors during light-off experiments with various noble metal-containing catalysts (2–4). However, simple calculations show that there are no contradictions. The amount of linear CO species on the used Pt/Al_2O_3 catalyst (after several pretreatments) measured at 300 K with a mass spectrometer (12) during a switch He → 2% CO/3% Ar/He is ≈50 μmol/g (30). The weight of catalyst used in the FTIR experiments is ≈40 mg, indicating that at 300 K there is ≈2 μmol of L species in the IR-cell reactor. With a 2% O_2/He mixture, Fig. 1 shows that the coverage decreases from 1 to 0.5 in ≈80 s. This gives an initial rate of disappearance of L species of ≈0.012 μmol/s. This value must correspond to the highest rate of CO_2 production at 300 K with a 1% CO/2% O_2/He mixture considering that the rate of adsorption of CO is not the limiting step. The CO molar flow rate during the light-off test is 1.40 μmol/s (200 cm^3/min of the reactive mixture). This value is strongly higher that the rate of CO_2 production (0.012 μmol/s) and indicates that the highest CO conversion at 300 K is ≈0.8%. This is in agreement with the fact that the light-off tests on Pt-containing solids always indicate a very low conversion before 373 K (2–4). In a following study we show that the kinetic parameters determined above for steps S3 and S2 and for step S1 in (11, 12) allow us to interpret the evolution of the coverage of the L species and correlatively of the CO conversion during light-off tests with several reactive mixtures 1% CO/x% O_2/He with x in the range (0.125–50).

3.8. Evolution of the Coverage of the L Species during Its Oxidation for $\theta_L < 0.2$

The straight lines in Fig. 6 are mainly obtained for $\theta_L > 0.2$. For lower θ_L values (not shown) the slopes change for the lower P_{O_2} values. This has also been observed by Cant and Donaldson (31) for the oxidation of the L species on Pt/SiO_2 catalysts. Due to the experimental procedure these authors lost the main contribution of the decrease in the coverage of the L species and their data only concern θ_L values in the range 0.3–0.1. Under these conditions $\ln(\theta_L) = f(t)$ was not linear and the authors considered that this was due to a dependence of the activation energy of step S3 on θ_L. They assumed (31) that the rate of disappearance of the L species was given by an equation similar to Elovich's equation, with an activation energy given by $E_0 - \alpha\ \theta_L$ with $\alpha = 50$ kJ/mol. They determined an apparent activation energy of 48 kJ/mol at $\theta_L = 0.2$ leading to E_0 of 58 ± 6 kJ/mol which can be compared to $E_a = 65$ kJ/mol found above. Note that the mathematical treatment used by Cant and Donaldson (31) did not consider the effect of the change in the oxygen coverage during the removal of the L species. Thus, their data were implicitly treated in the absence of competition between the L and O_{ads} species as in the present study. Moreover, Cant and Donaldson (31) indicate a small positive order dependence on oxygen pressure on the rate of oxidation in agreement with the value of 0.5 determined in the present study. The various straight lines in Fig. 6 for $\ln \theta_L = f(t)$ at several oxygen partial pressures lead to the conclusion that the apparent activation energy of step S3 is constant in the range 1–0.2. However, in agreement with the observations of Cant and Donaldson (31) the slopes change for $\theta_L < 0.2$ and for low P_{O_2} values. We consider that this is due to an increase in the activation energy of step S3 as suggested in (31). However, we do not use the formalism of Elovich's equation (31) because it does not take into account the coverage of the oxygen. We only introduce a variation of the activation energy of step S3; $E_3 + \alpha\theta_L$ where E_3 is the constant activation energy between $1 < \theta_L < 0.2$ and α (in kJ/mol) is the increasing factor for $\theta_L < 0.2$. The evolution of θ_L with time on stream is given by

$$\frac{-d\theta_L}{dt} = \frac{k \cdot T}{h} \cdot \exp - \left(\frac{E_3 + \alpha \cdot \theta_L}{R \cdot T} \right) \cdot \theta_L \cdot \sqrt{K_{O_2} \cdot P_{O_2}}, \quad [5]$$

where K_{O_2} is given by expression [4] with $E_{O_2} = 30$ kJ/mol. Figure 11 compares the experimental curves $\theta_L = f(t)$ for three oxygen partial pressures (Fig. 11, ▲, ■, ●) to the theoretical curve obtained by solving Eq. [5]. Curves d, e, and f are obtained with $E_3 = 75 \pm 2$ kJ/mol and $\alpha = 0$. The comparison between curves a–c (▲, ■, ●) and d–f shows that (i) the activation energy of step S3 is constant for $\theta_L > \approx 0.2$, and (ii) for $\theta_L < \approx 0.2$ the theoretical curves (d, e) are lower

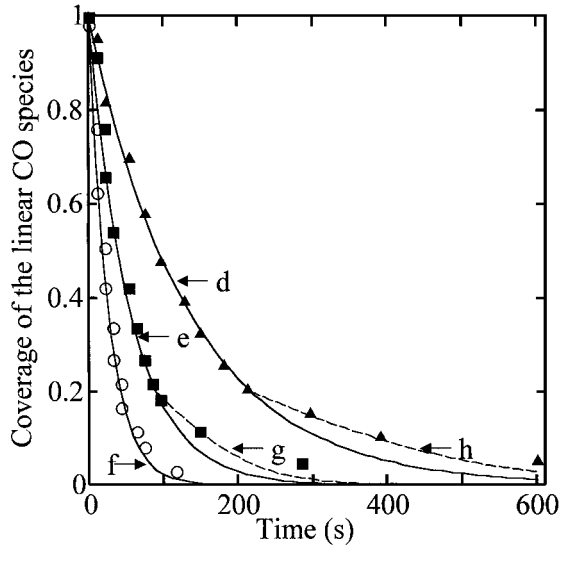

FIG. 11. Comparison of the coverage of the L species during its oxidation at 298 K for three oxygen partial pressures with the theoretical curves obtained from Eq. [5]: (a–c) experimental coverages for (▲, a) $P_{O_2} = 0.5 \times 10^3$ Pa; (■, b) $P_{O_2} = 8 \times 10^3$ Pa; (●, c) $P_{O_2} = 16 \times 10^3$ Pa; (d–f) theoretical coverages according to Eq. [5] for the three P_{O_2} values with $E_3 = 75 \pm 2$ kJ/mol and $\alpha = 0$; (h and g) theoretical coverages considering $\alpha = 10$ kJ/mol in Eq. [5] for $\theta_L < 0.2$.

than the experimental data for $P_{O_2} > 8 \times 10^3$ Pa (curves a and b). Note the good agreement between the theoretical curve and the experimental data for $P_{O_2} = 16 \times 10^3$ Pa for all the θ_L values (same results for $P_{O_2} = 10^5$ Pa) and that the value of E_3 used in Eq. [5] is in the range of values 65–80 kJ/mol determined above. Curves g and h give the theoretical curves considering an increase in the activation energy of step S3 with the decrease in θ_L using $\alpha = 10$ kJ/mol for $\theta_L <\approx 0.2$ The better accord between curves g and h and the experimental data confirms that the activation energy of steps S3 slightly increases with the decrease of θ_L. However, this variation of E_3 appears as a function of the oxygen partial pressure because the activation energy of step S3 is constant in the θ_L range 1–0.06, for P_{O_2} values $>8 \times 10^3$ Pa (curves c and f). It seems that a higher amount of oxygen leads to a constant value for E_3 with θ_L.

4. CONCLUSION

The following conclusions are derived from the present study on a Pt/Al_2O_3 catalyst.

(a) The linear adsorbed CO species (denoted by L) on Pt sites is oxidized in CO_2 at a temperature lower than 350 K in the presence of x% O_2/He mixture with x in the range 0.5–100 and a total pressure of 1 atm.

(b) The oxidation of the L species follows the Langmuir–Hinselwood mechanism with an O_{ads} species formed by the dissociative chemisorption of oxygen. The Eley–Rideal mechanism does not operate. The elementary step (denoted by S3) which controls the oxidation of the L species is

$$L + O_{ads} \rightarrow CO_{2\,ads},$$

with a rate constante k_3 and an activation energy E_3.

(c) There is no competition between L species and the adsorbed oxygen species O_{ads}: each species is adsorbed on different sites (no competition of adsorption).

(d) The O_{ads} species is weakly adsorbed and its adsorption (step S2) is considered at the equilibrium.

(e) The apparent rate constant of step S3 is $k_a = k_3(K_{O_2}P_{O_2})^{0.5}$, where K_{O_2} is the adsorption coefficient of O_2. The apparent activation energy is 65 kJ/mol and the heat of adsorption of O_2 is estimated $<\approx$30 kJ/mol.

(f) The activation energy of step S3 is in the range 65–80 ($\pm$3) kJ/mol and the preexponential factor of the rate constant k_3 is $\approx 10^{13}$ s^{-1} at $T > 350$ K, in agreement with that expected from statistical thermodynamics.

(g) The rate of oxidation of the L species is in qualitative agreement with the CO conversion during light-off tests performed at temperatures lower than 370 K.

(i) For θ_L values lower than 0.2 and for oxygen partial pressure lower than 16×10^3 Pa, the activation energy of step S3 increases slightly with the decrease in θ_L.

In subsequent studies it is shown that the above kinetic parameters for steps S2 and S3 allow us to explain the change in the coverage of the L species and correlatively the evolution of the CO conversion during light-off tests in the range 300–740 K using several 1% CO/x% O_2/He with x in the range 0.125–50.

ACKNOWLEDGMENT

We acknowledge with pleasure FAURECIA Industries, Bois sur Prés, 25 550 Bavans, France, for its financial support.

REFERENCES

1. Nibbelke, R. H., Campman, M. A. J., Hoebink, J. H. B. J., and Marin, G. B., *J. Catal*. **171**, 358 (1997).
2. Wojciechowski, B. W., and Aspey, S. P., *Appl. Catal. A* **190**, 1 (2000).
3. Herz, R. H., and Marin, S. P., *J. Catal*. **65**, 281 (1980).
4. Harold, M. P., and Garske, M. E., *J. Catal*. **127**, 524 (1991).
5. Cai, Y., Strenger, H. G., Jr., and Lyman, C. E., *J. Catal*. **161**, 123 (1996).
6. Thormählen, P., Skoglundh, M., Fridell, E., and Anderson, B., *J. Catal*. **188**, 300 (1999).
7. Engel, T., and Ertl, G., *Adv. Catal*. **28**, 1 (1979).
8. Razon, L. F., and Schmitz, R. A., *Catal. Rev. Sci. Eng*. **28**, 89 (1986).
9. Shigeishi, R. A., and King, D. A., *Surf. Sci*. **75**, L 397, (1978).
10. Bowker, M., Jones, I. Z., Bennett, R. A., and Poulston, S., *Stud. Surf. Sci. Catal*. **116**, 431 (1998).
11. Szanyi, J., and Goodman, D. W., *J. Phys. Chem*. **98**, 2972 (1994).
12. Chafik, T., Dulaurent, O., Gass, J. L., and Bianchi, D., *J. Catal*. **179**, 503 (1998).
13. Dulaurent, O., and Bianchi, D., *Appl. Catal*. **196**, 271 (2000).
14. Dulaurent, O., Chandes, K., Bouly, C., and Bianchi, D., *J. Catal*. **188**, 237 (1999).
15. Dulaurent, O., Chandes, K., Bouly, C., and Bianchi, D., *J. Catal*. **192**, 262 (2000).
16. Dulaurent, O., Chandes, K., Bouly, C., and Bianchi, D., *J. Catal*. **192**, 273 (2000).
17. Dulaurent, O., Courtois, X., Perrichon, V., and Bianchi, D., *J. Phys. Chem. B* **104**, 6001 (2000).
18. Dulaurent, O., Bourane, A., Nawdali, M., and Bianchi, D., *Appl. Catal*. **201**, 272 (2000).
19. Bourane, A., Dulaurent, O., and Bianchi, D., *J. Catal*. **196**, 115 (2000).
20. Bourane, A., Dulaurent, O., and Bianchi, D., submitted for publication.
21. Haaland, D. M., and Williams, F. L., *J. Catal*. **76**, 450 (1982).
22. Lindstrom, T. H., and Tsotsis, T. T., *Surf. Sci*. **150**, 487 (1985).
23. Barshad, Y., Zhou, X., and Gulari, E., *J. Catal*. **94**, 128 (1985).
24. Kaul, D. J., and Wolf, E. E., *J. Catal*. **89**, 348 (1984).
25. Anderson, J. A., *J. Chem. Soc., Faraday Trans*. **88**, 1197 (1992).
26. Nibbelke, R. H., Nievergeld, A. J. L., Hoebink, J. H. B. J., Marin, G. B., *Appl. Catal. B* **19**, 245 (1998).
27. Sharma, S. B., Miller, J. T., and Dumesic, J. A., *J. Catal*. **148**, 198 (1994).
28. Sarkany, J., Bartok, M., and Gonzalez, R. D., *J. Catal*. **81**, 347 (1983).
29. Lévy, P. J., Pitchon, V., Perrichon, V., Primet, M., Chevrier, M., and Gauthier, C., *J. Catal*. **178**, 363 (1998).

30. Bourane, A., Dulaurent, O., and Bianchi, D., *J. Catal*. **195**, 406 (2000).
31. Cant, N. W., and Donaldson, R. A., *J. Catal*. **71**, 320 (1981).
32. Pavlova, S. N., Sadykov, V. A., Razdobarov, V. A., and Paukshtis, E. A., *J. Catal*. **161**, 507 (1996).
33. Li, Y., Boecker, D., and Gonzalez, R. D., *J. Catal*. **110**, 319 (1988).
34. Xu, J., and Yates, J. T., Jr., *J. Chem*. *Phys*. **99**, 725 (1993).
35. Somorjai, G. A., "Chemistry in Two Dimensions." Cornell Univ. Press, Ithaca, NY, 1981.
36. Wartnaby, C. E., Stuck, A., Yeo, Y. Y., and King, D. A., *J. Chem*. *Phys*. **102**, 1855 (1995).
37. Glasstone, S., Laidler, K. J., and Eyring. H., "The Theory of Rate Processes." McGraw-Hill, New York, 1941.
38. Laidler, K. J., *Catalysis* **1**, 75 (1954).
39. Coulston, G. W., and Haller, G. L., *ACS Symp. Ser.* **482**, 59 (1992).
40. Pacia, N., Cassuto, A., Pentenero, A., and Weber, B., *J. Catal*. **41**, 455 (1976).